Available online at www.sciencedirect.com
ScienceDirect
Journal of Power Sources 178 (2008) 807–814
JOURNAL OF POWER SOURCES
www.elsevier.com/locate/jpowsour

Short communication

Morphological characterization of $LiFePO_4$/C composite cathode materials synthesized via a carboxylic acid route

George Ting-Kuo Fey *, Tung-Lin Lu

Department of Chemical and Materials Engineering, National Central University, Chung-Li 32054, Taiwan, ROC

Received 12 July 2007; received in revised form 20 August 2007; accepted 14 September 2007
Available online 21 September 2007

Abstract

A new type of $LiFePO_4$/C composite surrounded by a web containing both amorphous and crystalline carbon phases was synthesized by incorporating malonic acid as a carbon source using a high temperature solid-state method. SEM, TEM/SAED/EDS and HRTEM were used to analyze surface morphology and confirmed for the first time that crystalline carbon was present in $LiFePO_4$/C composites. The composite was effective in enhancing the electrochemical properties such as capacity and rate capability, because its active component consists of nanometer-sized particles containing pores with a wide range of sizes. An EDS elemental map showed that carbon was uniformly distributed on the surface of the composite crystalline particles. TEM/EDS results clearly show a dark region that is $LiFePO_4$ with a trace of carbon and a gray region that is carbon only. To evaluate the materials' electrochemical properties, galvanostatic cycling and conductivity measurements were performed. The best cell performance was delivered by the material coated with 60 wt.% malonic acid, which delivered first cycle discharge capacity of 149 mAh g^{-1} at a *C*/5 rate and sustained 222 cycles at 80% of capacity retention. When carboxylic acid was used as a carbon source to produce $LiFePO_4$, overall conductivity increased from 10^{-5} to 10^{-4} S cm^{-1}, since particle growth was prevented during the final sintering process.

Keywords: Li-ion batteries; $LiFePO_4$; Carbon; Composite; Malonic acid; Morphology

1. Introduction

In the search for low cost, environmentally friendly, and highly safe cathode materials, the $LiFePO_4$/C composite has emerged as a promising candidate for lithium-ion batteries in large-size and high-rate applications such as power tools and hybrid electric vehicles [1,2]. The composite has several advantages which attracted our attention: (1) a high theoretical capacity of 170 mAh g^{-1} [3]; (2) the natural abundance and nontoxicity of iron [4]; (3) excellent thermal stability [5,6]; (4) significant electronic conductivity enhancement [3,7–9]; (5) a tremendous increase in Li-ion diffusivity [10]. The intrinsic weaknesses of $LiFePO_4$, such as low electronic conductivity (10^{-8} to 10^{-10} S cm^{-1}) and slow Li^+ diffusion kinetics, have been overcome using three effective methods: selective doping with supervalent cations [10–13], particle-size reduction [4,14], and intimate carbon coating around the particles via suitable preparation routes [3,8,14,15]. The ion doping method can increase the lattice electronic conductivity or chemical diffusion coefficient of lithium within the crystal, but when the carbon coating method increases non-lattice electronic conductivity, it is accompanied by a loss in energy density due to the electrochemically inert additive. Conductivity can be enhanced significantly by either adding carbon to the $LiFePO_4$ matrix [3,16], or by surface coating $LiFePO_4$ particles with thin layers of carbon [17–20], provided that the particle size and particle distribution of $LiFePO_4$/C composites are well controlled.

Over the past decade, many efforts have been devoted to enhancing the electrode capacity, rate capability, and electrochemical properties of $LiFePO_4$ materials through various synthetic and analytical techniques. Many soft chemistry routes, such as sol–gel synthesis [21], co-precipitation [22], hydrothermal reaction [23], and emulsion-drying method [24], have been tested to evaluate how to make a good carbon coating and to control the particle size. In this work, we adopted a high temperature solid-state method for the synthesis because it is widely used for mass production of chemicals. Despite knowing that carbon can

* Corresponding author. Tel.: +886 3 425 7325; fax: +886 3 425 7325.
E-mail address: gfey@cc.ncu.edu.tw (G.T.-K. Fey).

0378-7753/$ – see front matter © 2007 Elsevier B.V. All rights reserved.
doi:10.1016/j.jpowsour.2007.09.039

improve capacity and rate capability, it is still not clear how and why it does.

In this paper, we attempted to coat carbon by incorporating malonic acid as a carbon source, and to understand the effect of carbon coating on cell performance.

To our knowledge, no fully characterized $LiFePO_4$/C composite morphology investigation has been conducted so far. We first present the morphological characterization of the obtained carbon coating of $LiFePO_4$/C composites and then describe their microstructure, electrochemical properties and cell performances as cathode materials.

2. Experimental

Details of the synthesis, characterization, and cell performance of $LiFePO_4$/C composite materials prepared by the carboxylic acid-assisted solid-state method are provided in our previous work in Ref. [25]. The $LiFePO_4$/C composite was synthesized using lithium carbonate, iron(II) oxalate dihydrate, and ammonium dihydrogen phosphate in a stoichiometric molar ratio (1.03:1:1) by a high temperature solid-state method. The preparation involved two heating steps. The preliminary heating was for preparing the precursor and the subsequent heating was for preparing the product. The reactants for preparing the precursor were mixed by ball milling in acetone for 3 h. The resulting gel was dried at 60 °C in a furnace under Ar flowing, thoroughly ground, and heated at 250 °C h^{-1} to 320 °C under purified Ar/H_2 (vol. 95:5) gas for 10 h. Carboxylic acid was employed as a carbon source in the composite formation, which was added to the precursor before the second grinding step. The weight % of carboxylic acid was defined as the ratio of the weight of carboxylic acid to the weight of $LiFePO_4$ precursor. Malonic acid (propandioic acid, $HOOCCH_2COOH$) and salicylic acid (2-hydroxybenzoic acid, $C_6H_4(OH)(COOH)$) were used in this work. After the precursor was mixed well with carboxylic acid powders, the mixture was thoroughly ground. The final composite product was obtained by heating the mixture at 250 °C h^{-1} to 600 °C for 12 h under purified Ar/H_2 (vol. 95:5) gas.

Electrochemical experiments were carried out with coin type cells of the 2032 configuration and were assembled in an argon-filled VAC MO40-1 glove box in which the oxygen and water contents were maintained below 2 ppm. The cathodes for electrochemical studies were prepared by a doctor-blade coating method with a slurry of 85 wt.% carbon-coated $LiFePO_4$ powder, 10 wt.% conductive carbon black and 5 wt.% poly(vinylidene fluoride) as a binder, in *N*-methyl-2-pyrrolidone (NMP), as the solvent for the mixture, which was then applied onto an etched aluminum foil current collector and dried at 393 K for 12 h in an oven. Lithium metal (Foote Mineral) was used as the anode and a 1 M $LiPF_6$ in ethylene carbonate:diethyl carbonate (EC:DEC) (1:1, v/v) (Tomiyama Chemicals) was used as the electrolyte with a Celgard membrane as the separator. The cells charge–discharge cycles were preformed at a *C*/5 rate between 2.8 and 4.0 V using a multi-channel battery tester (Maccor 4000). Phase transitions during the cycling processes were examined by a slow scan cyclic voltammetric experiment. The cells for the cyclic voltammetric studies were assembled inside the glove box with lithium metal foil serving as both counter and reference electrodes. The electrolyte used was the same as that for the coin cell. Cyclic voltammograms were run on a Solartron 1287 Electrochemical Interface at a scan rate of 0.05 mV s^{-1} between 3.0 and 4.0 V.

The morphology of $LiFePO_4$/C composite was observed by scanning electron microscope (SEM; Hitachi S-3500 V) and high resolution transmission electron microscope (HR-TEM; Jeol TEM-2000FXII). The carbon distribution was confirmed with energy dispersive spectroscopy (Energy Dispersive X-ray Spectrometry). The Raman microscope system (ISA T64000) was used to observe individual particles of carbon in the range of 800–1750 cm^{-1}. The excitation wave length was supplied by an internal Ar ion 10 mW laser. The conductivity was measured by four-point conductivity measurements of a Keithley Model 2400S source meter.

3. Results and discussion

The X-ray powder diffraction patterns of $LiFePO_4$ uncoated and coated with 60 wt.% malonic acid after firing at 600 °C have been reported elsewhere [25]. A single-phase $LiFePO_4$ with an ordered olivine structure indexed by orthorhombic *Pnmb* (JCPDS card no. 40-1499) appeared in all the samples and there were no impure phases of Fe_2O_3 and $Li_3Fe_2(PO_4)_3$ [14]. As temperatures rose, the diffraction peaks became slightly sharper, which indicates that crystallinity improved [26,27]. However, no crystalline or amorphous carbons were detected in the XRD patterns, because the formed carbon was too small or too thin on the $LiFePO_4$ particles.

In $LiFePO_4$/C, carbon distribution and carbon morphology affect its electrochemical performance [11,28,29]. Fig. 1 displays a SEM image and four corresponding EDS maps of phosphorous, carbon, iron and oxygen in $LiFePO_4$ coated with 60 wt.% malonic acid. The EDS carbon map shows a uniform distribution of carbon in the sample on the surface of the composite particles. There is no remarkable segregation of carbon in the mapping area, which indicates that carbon is uniformly coated on the surface of $LiFePO_4$ grains. The SEM image shows that the synthesized $LiFePO_4$/C powders are mainly fine particles between 100 and 200 nm in size, although a few large particles up to 1 μm exist.

In order to observe the carbon morphology in detail, we studied this composite material further by TEM/SAED/EDS techniques. A 200-mesh copper grid coated with a silicon monoxide film instead of carbon to ensure that any carbon detected was from the sample. Our selection of grid avoids any controversy that carbon could have come from the grid, although Cu and Si peaks were present as impurities or background in the EDS spectrum.

Fig. 2a is a TEM micrograph of $LiFePO_4$ coated with 60 wt.% malonic acid. The image shows carbon-like nanometer-sized webs wrapped around and connecting the $LiFePO_4$ particles, which help enhance electrochemical performance. The $LiFePO_4$ crystallites appear as the darker regions, known as the particles, while the carbon coatings surround the primary particles as the

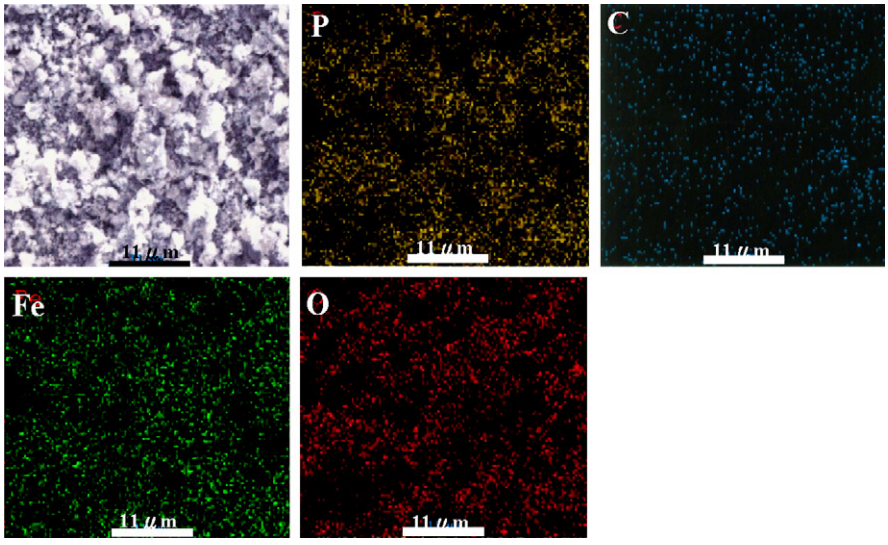

Fig. 1. A SEM image and the corresponding EDS maps of carbon, iron, oxygen, and phosphorus in $LiFePO_4$ coated with 60 wt.% malonic acid.

grayish regions, known as the webs. The SAED pattern in Fig. 2b confirms that the particles are crystalline due to the presence of bright spots and the SAED pattern in Fig. 2c shows that the webs are amorphous due to the presence of hollow rings. To clarify their identity, we carried out some EDS analysis. The results are shown in Fig. 2d and e. They definitely indicate that the particles are crystalline $LiFePO_4$ and the webs are amorphous carbon only. There is also a small carbon peak in Fig. 2d, probably due to the carbon thin film on the particles. It is not clear at this point whether the structure of the carbon thin film is amorphous or crystalline, but it appears critical to cathode performance. Since the selected area of the web in Fig. 2a is located more than 200 nm away from the $LiFePO_4$ particles, it prompted us to expand our study to include all the areas that were close to the particles.

The sample used in Fig. 2 was studied further and those results are illustrated in the three distinct areas of Fig. 3. The TEM image in Fig. 3a provides a representative general profile of the sample, while Fig. 3b–d are magnified images. Fig. 3d is a close-up of the crystalline $LiFePO_4$ particles which are obviously very regular in shape. The gap separating the two-circled areas in Fig. 3b is shorter than the respective gap highlighted in Fig. 3c. The EDS/SAED spectra in Fig. 3e and g confirm that the darker regions were crystalline $LiFePO_4$, but what is more interesting is that the similar looking spectra in Fig. 3f and h both indicate the presence of two types of carbon in the grayish regions of Fig. 3b and c, respectively. The webs in Fig. 3c are amorphous carbon, but the ones in Fig. 3b have a trace of crystalline carbon, because they were relatively closer to the particle than the webs in Fig. 3c. This observation led us to investigate whether the webs' proximity to the particles affected the structure of the carbon. However, there was a slight difference in the SAED patterns of Fig. 3j and l. Fig. 3j displayed a few weak spots in addition to a hollow ring, while Fig. 3l only displayed a hollow ring. The presence of spots in the SAED pattern indicates that some crystalline materials were present.

Similar to the "like dissolves like" concept in solution chemistry, we believe that part of this principle may be applicable

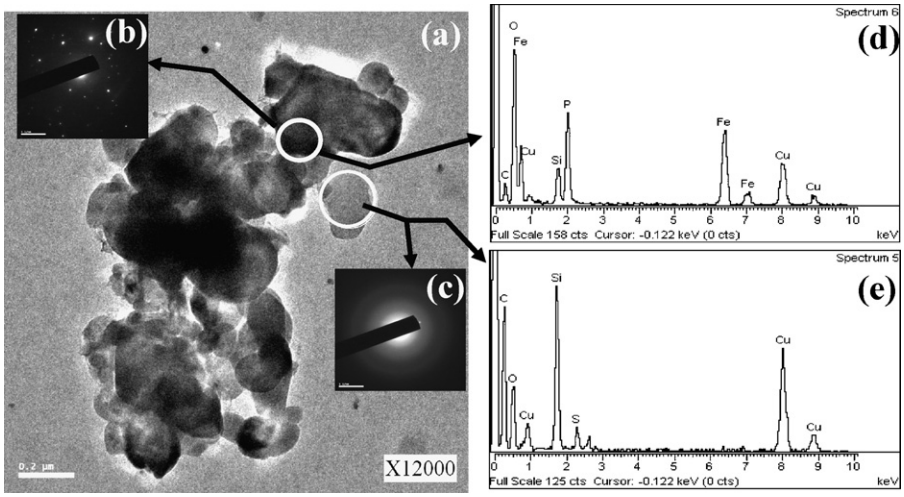

Fig. 2. (a) A TEM micrograph of $LiFePO_4$ coated with 60 wt.% malonic acid; (b and c) SAED and (d and e) EDS analyses for the particles.

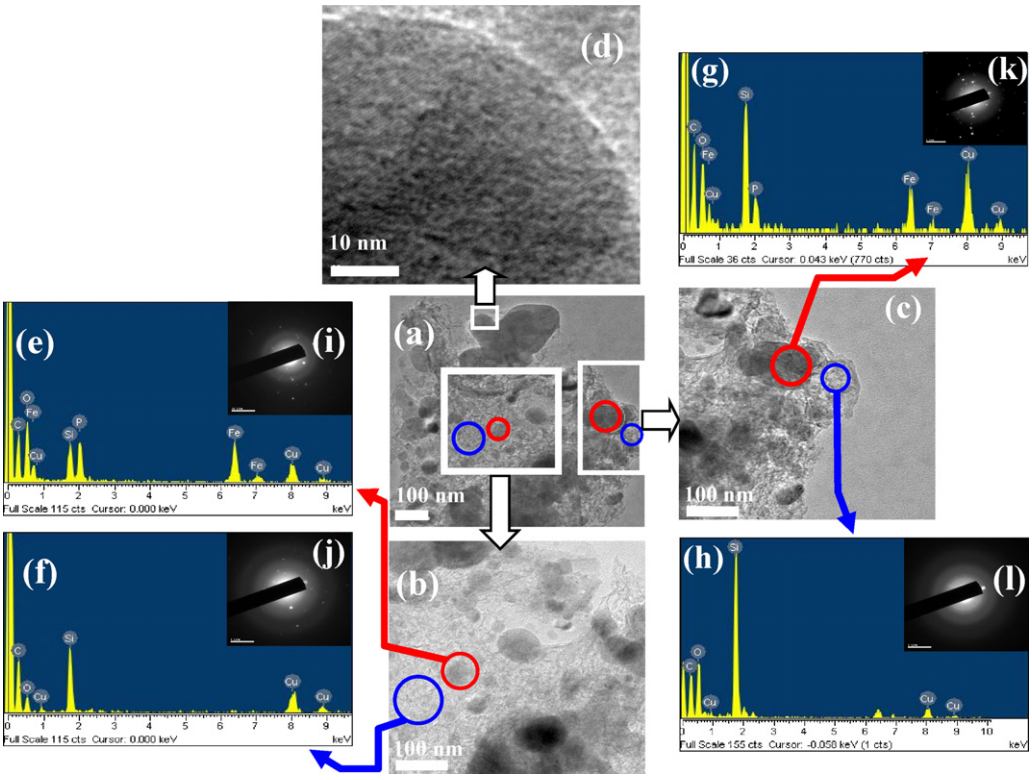

Fig. 3. (a–d) TEM micrographs of $LiFePO_4$ coated with 60 wt.% malonic acid; (e–h) EDS analyses for the particles; (i–l) SAED patterns for the particles.

in materials morphology. Materials that can assume different structures will tend evolve into a structure that is similar to the materials that are located closest to them: our theory is that "like influences like". For example, carbon that is located closer to a crystalline $LiFePO_4$ structure will tend to assume a partially crystalline carbon structure. In contrast, a carbon that is very far away becomes amorphous because it is too far away to be influenced by the crystalline $LiFePO_4$ and therefore assumes a random or amorphous structure.

To ensure this was not simply an anomaly, we prepared the composite material using salicylic acid as a carbon source. Fig. 4 is a TEM micrograph of $LiFePO_4$ coated with 50 wt.% salicylic acid. Fig. 4b is a magnified image of the outlined area in Fig. 4a. The sections indicated by I and II were selected in order to compare their carbon structure. The EDS spectra in Fig. 4c and d confirm that the darker region was $LiFePO_4$ and the grayish region was carbon, respectively. The SAED patterns in Fig. 4f and g also show that there are two types of carbon: the com-

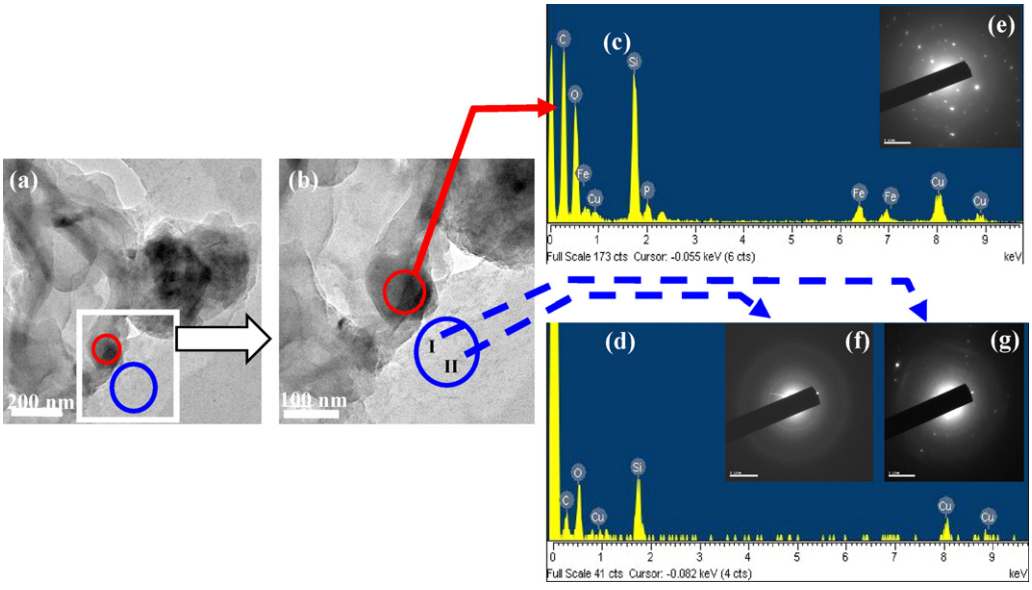

Fig. 4. (a and b) TEM micrographs of $LiFePO_4$ coated with 50 wt.% salicylic acid; (c and d) EDS analyses for the particles; (e–g) SAED patterns for the particles.

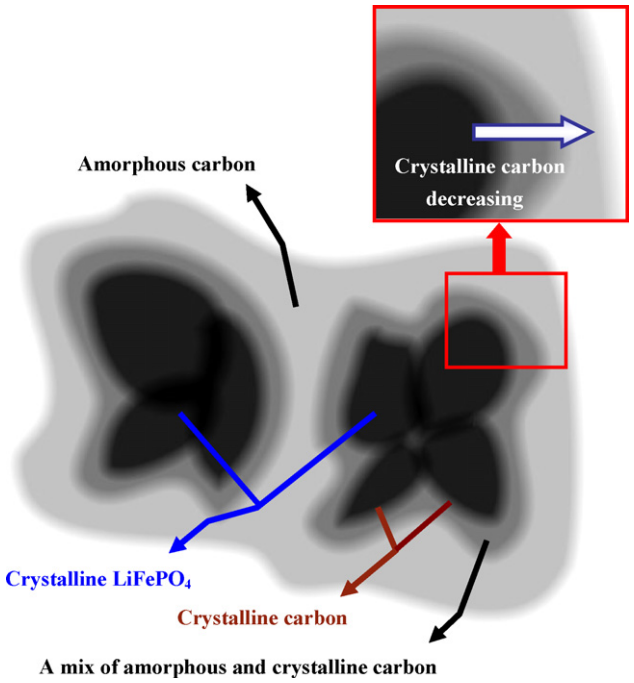

Fig. 5. A schematic diagram illustrating how carbon is distributed and coated on the $LiFePO_4$ particles.

pletely amorphous carbon in section II, located farther from the $LiFePO_4$ particle, and the amorphous carbon mixed with trace crystalline carbon in section I, located closer to the particle, respectively. These additional morphology results support our results from when we used malonic acid as a carbon source.

Based on our "like influences like" theory, a schematic diagram suggesting how carbon is distributed and coated on the $LiFePO_4$ particles is depicted in Fig. 5. The diagram is broken down into three sections of carbons. The first is the crystalline carbon coating on the surface of the composite material. The second is a mix of amorphous and trace crystalline carbon closer to the particles. The third is completely amorphous in the area furthest away from the particles. In order to verify the above model, using the same TEM sample, we carefully selected the appropriate sample area for TEM/EDS analysis. Fig. 6a and b are the TEM micrographs for the areas very close to the crystalline $LiFePO_4$ region. High resolution tunneling electron microscopy (HRTEM) was performed on the powder sample to examine the fine structure of the synthesized $LiFePO_4$/C composite. The HRTEM micrograph in Fig. 6c clearly shows that there is a small crystalline region between the interstitial grain-boundary of carbon and $LiFePO_4$. Although the crystallites in this small crystalline region cannot be identified because it is too small to be analyzed by EDS, the carbon and $LiFePO_4$ crystalline images can be easily discerned. HRTEM of thin particle edges revealed that carbon was deposited on the planes of orthorhombic $LiFePO_4$ and formed a 1–2 nm thick crystalline region in the interstitial grain boundary between carbon and $LiFePO_4$ (Fig. 6c). The TEM micrograph in Fig. 7a consists of two parts: a dark region and a grayish region which surrounds it. Interestingly, both the SAED patterns in Fig. 7b and c indicate that the studied materials are a crystalline phase. The EDS results from Fig. 7d and e unambiguously show that the particles in the dark region are $LiFePO_4$ with a trace of carbon and those in the grayish region are carbon only. To the best of our knowledge, this is the first report to confirm the presence of crystalline carbon in the $LiFePO_4$/C composite. We feel that this could be significant since the conductivity of crystallite carbon is greater than amorphous carbon. The presence of evenly distributed carbon enhanced electronic conductivity. Moreover, carbon particles between $LiFePO_4$ particles can prevent particle coalescence. The magnified image of Fig. 7a reveals that the whole $LiFePO_4$ powder is covered with crystalline carbon. The small crystalline and porous agglomerate structure of $LiFePO_4$ also facilitates lithium ion diffusion during insertion/extraction processes by providing short pathways and reducing cell resistance in the active material crystal.

Fig. 8 shows the cyclic voltammetry (CV) profiles of the $LiFePO_4$/C composite electrode for the 1st, 2nd, 5th and 10th cycles measured between 3.0 and 4.0 V to identify the characteristics of the redox reactions in Li-ion cells. The reduction and oxidation peak positions for the 1st, 2nd, 5th and 10th cycles of the $LiFePO_4$/C composite material are the same, at 3.26 and 3.74 V, respectively, which demonstrates that the Fe^{2+}/Fe^{3+} redox pairs contribute to the gain and loss of electrons in $LiFePO_4$/C crystal structure during the lithium insertion and extraction process.

Table 1 compares the capacity performance of various $LiFePO_4$/C composite materials. The capacity of the $LiFePO_4$/C electrode from this work was determined to be between 2.8 and 4.0 V by galvanostatic charge/discharge testing at a *C*/5 rate. The cycling conditions used in the cited references were at lower discharge rates, higher charge voltages, or wider voltage ranges

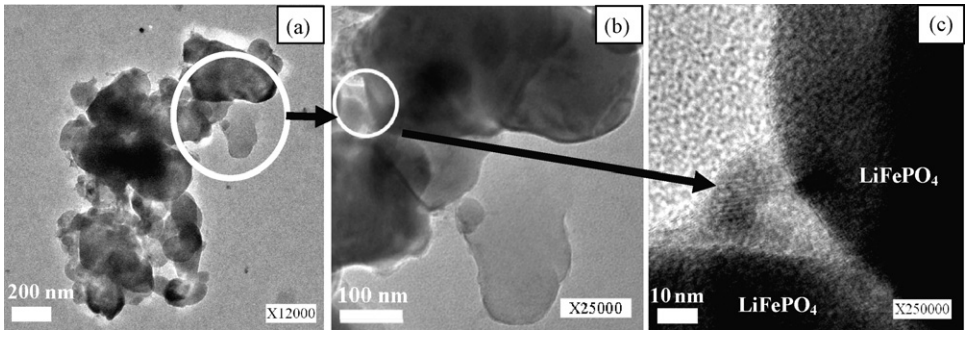

Fig. 6. (a and b) TEM micrographs of $LiFePO_4$ coated with 60 wt.% malonic acid; (c) a HRTEM image of $LiFePO_4$ crystals.

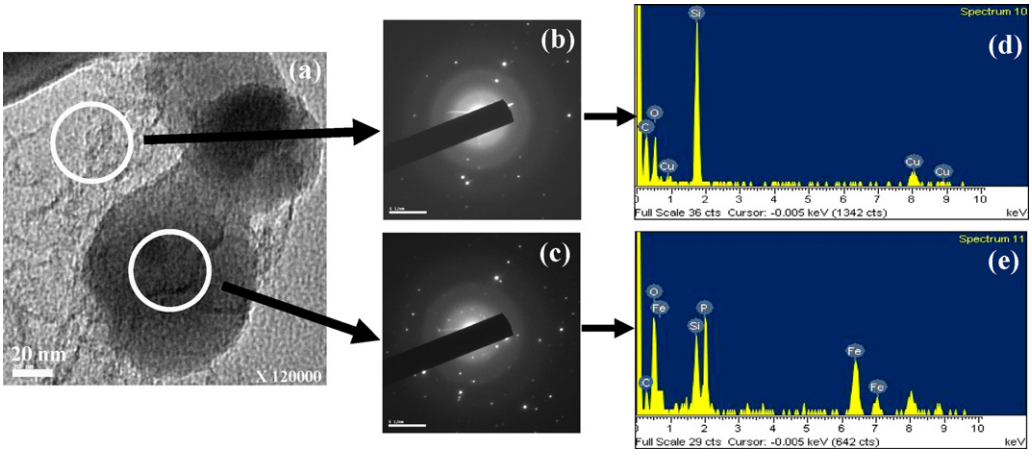

Fig. 7. (a) A TEM micrograph of $LiFePO_4$ coated with 60 wt.% malonic acid; (b and c) SAED patterns for the particles; (d and e) EDS analyses for the particles.

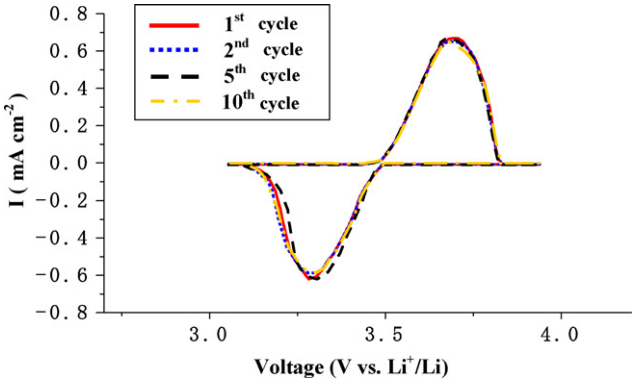

Fig. 8. Cyclic voltammetry of $LiFePO_4$ synthesized with 60 wt.% malonic acid at different cycle numbers. Scan rate = 0.05 mV s^{-1}; voltage range = 3.0–4.0 V.

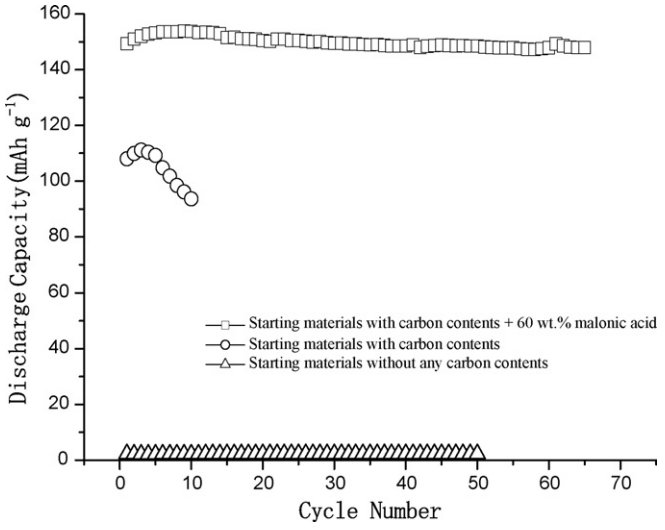

Fig. 9. Cyclability of $LiFePO_4$ synthesized with 60 wt.% malonic acid at a *C*/5 rate.

than in our study. Since all these conditions favor achieving a higher capacity, our sample actually demonstrated better capacity than those reported in previous literature. Fig. 9 shows the cycle performance of the un-coated and coated $LiFePO_4$ cathode materials. The uncoated ones included two types of $LiFePO_4$ materials: one was synthesized using the starting materials with carbon contents, as described in the synthesis section, and the other using the starting materials without any carbon contents. As expected, the former provided very poor cycle performance, while the latter showed virtually no capacity. The $LiFePO_4$/C composite material coated with 60 wt.% malonic acid displayed the best cycle performance [25]. A first cycle discharge capacity of 149 mAh g^{-1} at a *C*/5 rate was obtained by the coated material. The discharge capacities gradually increased in subsequent cycles, reached a maximum at 152 mAh g^{-1} after 20 cycles, and then stabilized. Even in the 222nd cycle, discharge capacity remained at 119 mAh g^{-1}, with 80% charge retention. The long cycle life of this composite cathode also confirmed

Table 1
Comparison of the capacity performance of $LiFePO_4$ composite materials

Starting materials	Carbon source	Method	Condition	Capacity (mAh g^{-1})	Reference
$FeC_2O_4{\cdot}2H_2O$, Li_2CO_3, $NH_4H_2PO_4$	Malonic acid	Solid state	2.8–4.0 V, 0.2 C rate	149	This work
$Fe(CH_3COO)_2$, $LiCH_3COO$, $NH_4H_2PO_4$	Resorcinol–formaldehyde carbon gel	Solid state	2.7–4.1 V, 0.1 C rate	158	[3]
$FeC_2O_4{\cdot}2H_2O$, $LiNO_3$, $NH_4H_2PO_4$	Citric acid	Sol–gel	3.0–4.0 V, 0.025 C rate	148	[30]
$Fe(NO_3)_3$, LiOH, H_3PO_4	Ascorbic acid	Sol–gel	3.0–4.1 V, 0.2 C rate	150	[31]
$C_6H_5FeO_7$, Li_3PO_4, H_3PO_4	Hydroxyethyl-cellulose	Sol–gel	2.7–4.1 V, 0.2 C rate	148	[32]
$FeC_2O_4{\cdot}2H_2O$, Li_2CO_3, $(NH_4)_2HPO_4$	High-surface area carbon black	Solid state	2.0–4.4 V, 0.2 C rate	152	[8]
$FeSO_4{\cdot}7H_2O$, Li_3PO_4, Na_3PO_4	Sucrose	Mechano-chemical activation	2.0–4.5 V, 0.05 C rate	160	[33]

good reversibility of the Fe^{2+}/Fe^{3+} redox behavior, as shown in Fig. 8.

The percentage of carbon in the composite by total organic carbon (TOC) or Raman spectral analysis was previously reported [25]. The actual carbon content of $LiFePO_4$ was 1.90 wt.% with the addition of 60 wt. % malonic acid. Although the as-synthesized material contained a considerable amount of carbon, it was necessary to add an additional amount of carbon during electrode preparation (in our case 10 wt.% of carbon black was added). The role of the additional carbon is probably twofold: (1) it ensures good inter-particle conductivity (the inherent thin carbon layer as shown in Fig. 6c is too thin for that purpose) and (2) it creates additional large pores in the electrode composite which are necessary for fast ion conduction at high operational rates.

As mentioned earlier, the thin carbon film or crystalline region on the surface of $LiFePO_4$ particles and between the interstitial grain-boundary of carbon and $LiFePO_4$ cannot be analyzed by EDS due to instrumental limitations. Micro Laser Raman spectroscopy is a useful technique for detecting carbon coating or the first layers at the surface of coated particles, since the penetration depth of the light inside the particles in Raman scattering is very small [2]. Accordingly, the appearance of two broad bands around 1358 and 1580 cm^{-1} itself is evidence that carbon thin film is coating the surface. Raman spectra were run on samples sintered with malonic and salicylic acids [25]. A relatively weak band appeared at 940 cm^{-1} that corresponds to the symmetric PO_4 stretching vibration of $LiFePO_4$. The peak intensity ratio (I_D/I_G) between 1358 and 1580 cm^{-1} broad bands was calculated in order to index the degree of carbon disordering. These two broad bands are often used as fingerprints of amorphous carbon films [29,34]. Compared to the bare $LiFePO_4$ sample ($I_D/I_G = 0.938$), the smaller I_D/I_G ratios for malonic (0.918) and salicyclic (0.907) acids are indicative of their greater conductivity with an improvement from 10^{-5} to 10^{-4} S cm^{-1} [25]. No direct relationship between electronic conductivity and carbon structure can be correlated with the peak intensity ratio and the band area ratio of the D versus G band. Apart from this, carbon source, content, and morphology also need to be taken into consideration. Nevertheless, cell performance in terms of discharge capacities and rate capability of $LiFePO_4$ cathodes can be correlated with proper amounts of sp^2-type carbon domains and a decreased level of disorder in graphene planes [2]. The electrochemical insertion/extraction properties of $LiFePO_4$/C composites are dependent on the powder morphology, particle size, impurity content, carbon source, and electronic conductivity of the materials [14,35,36].

4. Conclusions

$LiFePO_4$/C composites were synthesized using a carboxylic acid as a carbon source by a high temperature solid-state method. Studies via SEM, TEM/SAED/EDS and HRTEM analyses can provide insight into the morphology of $LiFePO_4$/C on a nanoscopic scale, which seems closely related to the preparation process of the samples. Our analyses also confirm the presence of crystalline carbon with $LiFePO_4$/C composites for the first time. A morphological model for $LiFePO_4$/C powders was proposed, based on the concept of "like influences like". This composite was effective in enhancing capacity and rate capability. $LiFePO_4$ coated with 60 wt.% malonic acid as a carbon source can deliver first discharge capacity of 149 mAh g^{-1} at a *C*/5 rate and sustain 222 cycles at 80% of capacity retention. The use of malonic acid as a carbon source not only increases the overall conductivity ($\approx 10^{-4}$ S cm^{-1}) of the material, but it also prevents particle growth during the final sintering process. By adopting a relatively high temperature solid-state method as described, it is possible to synthesize cathode materials on nanoscales that could accomplish high capacity retention and long cycle life. Narrow particle size distribution and better homogeneity of the carbon coating are important requirements in the search for high performance of cathode materials.

References

[1] G.W. Wang, S. Bewlay, J. Yao, J.H. Ahn, S.X. Dou, H.K. Liu, Electrochem. Solid State Lett. 7 (2004) A503.
[2] C.M. Julien, K. Zaghib, A. Mauger, M. Massot, A. Ait-Salah, M. Selmane, F. Gendron, J. Appl. Phys. 100 (2006) 063511.
[3] H. Huang, S.C. Yin, L.F. Nazar, Electrochem. Solid State Lett. 4 (2001) A170.
[4] F. Sauvage, E. Baudrin, L. Gengembre, J.M. Tarascon, Solid State Ionics 176 (2005) 1869.
[5] D.D. MacNeil, Z. Lu, Z. Chen, J.R. Dahn, J. Power Sources 108 (2002) 8.
[6] M. Takahashi, S.I. Tobishima, K. Takei, Y. Sakurai, Solid State Ionics 148 (2002) 283.
[7] Z. Chen, J.R. Dahn, J. Electrochem. Soc. 149 (2002) A1184.
[8] P.P. Prosini, D. Zane, M. Pasquali, Electrochim. Acta 46 (2001) 3517.
[9] R. Dominko, M. Gaberscek, J. Drofenik, M. Bele, S. Pejovnik, Electrochem. Solid State Lett. 4 (2001) A187.
[10] S.Y. Chung, J.T. Bloking, Y.M. Chiang, Nat. Mater. 1 (2002) 123.
[11] P.S. Herle, B. Ellis, N. Coombs, L.F. Nazar, Nat. Mater. 3 (2004) 147.
[12] J.F. Ni, H.H. Zhou, J.T. Chen, X.X. Zhang, Mater. Lett. 59 (2005)236.
[13] M. Abbate, S.M. Lala, L.A. Montoro, J.M. Rosolen, Electrochem. Solid State Lett. 8 (2005) A288.
[14] A. Yamada, S.C. Chung, K. Hinokuma, J. Electrochem. Soc. 148 (2001) A224.
[15] N. Ravet, J.B. Goodenough, S. Besner, M. Simoneau, P. Hovington, M. Armand, Electrochem. Soc. Abstr. 99–102 (1999) 127.
[16] A.K. Padhi, K.S. Nanjundaswamy, J.B. Goodenough, J. Electrochem. Soc. 144 (1997) 1188.
[17] K. Zaghib, K. Striebel, A. Guerfi, J. Shim, M. Armand, M. Gauthier, Electrochim. Acta 50 (2004) 263.
[18] N. Ravet, S. Besner, M. Simoneau, A. Vallee, M. Armand, J.F. Magnan, US Patent 6,855,273 B2 (2005).
[19] N. Ravet, Y. Chouinard, J.F. Magnan, S. Besner, M. Gauthier, M. Armand, J. Power Sources 97 (2001) 503.
[20] S.L. Bewlay, K. Konstantinov, G.X. Wang, S.X. Dou, H.K. Liu, Mater. Lett. 58 (2004) 1788.
[21] M. Piana, B.L. Cushing, J.B. Goodenough, N. Penazzi, Solid State Ionics 175 (2004) 233.
[22] P.P. Prosini, M. Carewska, S. Scaccia, P. Wisniewski, S. Passerini, M. Pasquali, J. Electrochem. Soc. 149 (2002) A886.
[23] S. Tajimi, Y. Ikeda, K. Uematsu, K. Toda, M. Sato, Solid State Ionics 175 (2004) 287.
[24] T.H. Cho, H.T. Chung, J. Power Sources 133 (2004) 272.
[25] G.T.K. Fey, T.L. Lu, F.Y. Wu, W.H. Li, International Conference on Materials for Advanced Technologies 2007, Singapore, July 1–6, 2007, J. Solid State Electrochem., in press.

[26] S.J. Kwon, C.W. Kim, W.T. Jeong, K.S. Lee, J. Power Sources 137 (2004) 93.
[27] C.H. Mi, X.B. Zhao, G.S. Cao, T.P. Tu, J. Electrochem. Soc. 152 (2005) A483.
[28] R. Dominko, M. Gaberscek, J. Drofenik, M. Bele, S. Pejovnik, J. Jamnik, J. Power Sources 119–121 (2003) 770.
[29] M.M. Doeff, Y. Hu, F. McLarnon, R. Kostecki, Electrochem. Solid State Lett. 6 (2003) A207.
[30] K.F. Hsu, S.Y. Tsaya, B.J. Hwang, J. Mater. Chem. 14 (2004) 2690.
[31] F. Croce, A. D'Epifanio, J. Hassoun, A. Deptula, T. Olczac, B. Scrosati, Electrochem. Solid State Lett. 5 (2002) A47.
[32] R. Dominko, M. Bele, M. Gaberscek, M. Remskar, D. Hanzel, S. Pejovnik, J. Jamnik, J. Electrochem. Soc. 152 (2005) A607.
[33] S. Franger, F.L. Cras, C. Bourbon, H. Rouault, Electrochem. Solid State Lett. 5 (2002) A231.
[34] Y. Yu, M.M. Doeff, R. Kostecki, R. Finones, J. Electrochem. Soc. 151 (2004) A1279.
[35] F. Croce, A.D. Epifanio, J. Hassoun, A. Deptula, T. Olezae, B. Scrosati, Electrochem. Solid State Lett. 5 (2002) A95.
[36] A.S. Andersson, B. Kalska, L. Haggstrom, J.O. Thomas, Solid State Ionics 130 (2000) 41.